A thermoregulation model for whole body cooling hypothermia

Ana Beatriz de C.G. e Silva[a,1,*], Luiz C. Wrobel[b], Fernando L.B. Ribeiro[a]

[a] *Civil Engineering Program,COPPE/Federal University of Rio de Janeiro Technological Center, Ilha do Fundão, CEP 21945-970, Rio de Janeiro, Brazil*
[b] *Institute of Materials and Manufacturing, Brunel University London, Uxbridge UB8 3PH, United Kingdom*

Abstract

This paper presents a thermoregulation model based on the finite element method to perform numerical analyses of brain cooling procedures as a contribution to the investigation on the use of therapeutic hypothermia after ischemia in adults. The use of computational methods can aid clinicians to observe body temperature using different cooling methods without the need of invasive techniques, and can thus be a valuable tool to assist clinical trials simulating different cooling options that can be used for treatment. In this work, we developed a finite element method (FEM) package using isoparametric linear three-dimensional elements which is applied to the solution of the continuum bioheat Pennes equation. Blood temperature changes were considered using a blood pool approach and a lumped analysis for intravascular catheter methods of blood cooling. Some analyses are performed using a three-dimensional mesh based on a complex geometry obtained from computed tomography medical images, considering a cooling blanket and an intravascular catheter. A comparison is made between the results obtained with the two techniques and the effects of each case in brain temperature reduction in a required period of time, maintainance of body temperature at moderate hypothermia levels and gradual

*Corresponding author
Email addresses: anabeatrizgonzaga@coc.ufrj.br (Ana Beatriz de C.G. e Silva), luiz.wrobel@brunel.ac.uk (Luiz C. Wrobel), fernando@coc.ufrj.br (Fernando L.B. Ribeiro)
[1] Tel.: +55 (21) 988406995

rewarming.

Keywords: thermoregulation, hypothermia, brain cooling, intravascular catheter, finite element method

1. Introduction

Therapeutic hypothermia is a medical treatment used to reduce the damages caused by ischemic diseases that lead to a hypoxic condition in the internal organs. The brain is the most vunerable organ to this condition [Tisherman and Sterz, 2005], which can be caused by cardiac arrest, arteries occlusion and cerebral trauma. After an hypoxic-ischemic event, also called primary phase of energy failure, cerebral oxidative metabolism is restored [Christiansen, Rakhilin, Tarakanova, and Wong, 2010]. However, a second energy failure phase may occur in the first few hours after the ischemia, and there is a critical time when secondary factors such as hypotension, hypoxia, hyperglycemia and hyperthermia may occur and cause brain cell damage [Hickey and J.Painter, 2006]. The window for hypothermic treatment occurs between the primary and secondary energy failure stages, and consists in reducing the brain temperature to a mild $(35-36^oC)$ or moderate $(32-35^oC)$ hypothermic state, depending on the type of intervention. This reduction results in a decrease of metabolic activities and other hazardous biochemical effects, offering protection and limiting the damage in the affected tissues.

In animal trials, an improvement of neurological sequels was observed after hypothermia treatment within six hours of injury [Eicher, Wagner, Katikaneni, Hulsey, Bass, Kaufman, Horgan, Languani, Bhatia, Givelichian, Sankaran, and Yager, 2005], even when only a small reduction $(1-2^oC)$ is achieved [Diao, Zhu, and Wang, 2003]. Nozari *et al.* [Nozari, Safar, Stezoski, Wu, Kostelnik, Radovsky, Tisherman, and Kochanek, 2006] state that mild or moderate hypothermia induced during cardiopulmonary resuscitation opens a window of

time to restore spontaneous circulation, minimizes organ injury and enables intact survival in dogs.

For adults, the most usual type of hypothermia treatment is whole body cooling (WBC) using thermal blankets and thermal mattresses, the application of ice pads, intracarotid infusion of cold fluid or intravascular catheter. The efficacy of each method is still under discussion, as there is no consensus so far about which of them would have a better effect in reducing sequels.

Multiple studies also suggest that, after the treatment, a gradual rewarming phase is really important. Zhu *et al.* [Zhu, Schappeler, Cordero-Tumangday, and Rosengart, 2009] state that rapid rewarming may result in rebound intracranial pressure elevation to dangerous levels and reduction of cerebral perfusion pressure, worsening outcome in brain injuries, emphasizing the importance of a gradual rewarming. For this reason, it is suggested that the process should be conducted at a rate of less than $0.5^oC/h$ [Hoque, Chakkarapani, Liu, and Thoresen, 2010].

In recent years, different models were developed to simulate the human thermoregulatory behaviour, from two-node models of core and skin heat balances to more complex multi-segment models of the human body and its thermoregulatory responses [Fiala, Lomas, and Stohrer, 1999]. The latter model incorporates concepts of physiological regulation to predict human thermal responses and body heat loss at various activity levels and thermal environments [Al-Othmani, Ghaddar, and Ghali, 2008]. Practical examples can be found in different applications [Kingma, Vosselman, Frijns, Steenhoven, and Lichtenbelt, 2014, Fiala, Lomas, and Stohrer, 1999, Al-Othmani, Ghaddar, and Ghali, 2008].

Early attempts to develop head cooling models did not consider arterial temperature changes [Dennis et al., 2003, Leeuwen et al., 2000]. According to Zhu and Diao [2001], the arterial temperature is the major determinant of the temperature in the body tissues, being responsible for a protective effect against external cooling. The blood flow in the circulatory system is responsible for the thermoregulation in the tissues. During hypothermia, hyperthermia or changes in the environment, it works regulating the local temperature [Bhowmik, Singh,

Repaka, and Mishra, 2013]. As the arterial temperature regulates the local tissue temperature, hypothermia simulation models must consider arterial temperature changes. The work of Al-Othmani *et al.* [Al-Othmani, Ghaddar, and Ghali, 2008] uses an arterial system model to calculate blood flow in the core tissue and a bioheat model to determine skin temperature for nude and clothed human bodies in transient non-uniform environments. The model presented in [Fiala, 1998] incorporates the body heat losses considering a non-uniform temperature distribution in the skin, regulatory responses, properties of clothing used and various environmental conditions such as extreme temperatures, wind speed and solar radiation. Xiang and Liu [Xiang and Liu, 2008] use a compartmental model of 12 body segments and a blood compartment to simulate whole body hyperthermia treatments for tumours. In [Laszczyk and Nowak, 2015b, Silva, Laszczyk, Wrobel, Ribeiro, and Nowak, 2016], a heat transfer model was implemented to simulate hypothermia treatment in neonates using a three-dimensional geometry obtained from magnetic resonance imaging (MRI) scans. In [Zhu, Schappeler, Cordero-Tumangday, and Rosengart, 2009], a numerical model for whole body intravascular cooling was developed and applied to a human body consisting of a cylinder of one material and a combination of components representing torso, head and limbs. The work calculated a $1.2^oC/hour$ cooling rate for a cooling capacity of $100W$ and suggested the method can be used to reduce critical fever of 40^oC or hypothermia of 34^oC in less than 3 hours.

For the rewarming phase of the hypothermia therapy, the simulation of the rewarming procedure by [Diao, Zhu, and Wang, 2003] considering a passive rewarming, taking off the helmet or icepacks and considering the room temperature of 25^oC, showed the need for more studies in this part of the procedure, as the passive rewarming in this case was too rapid. Some studies using a mattress to simulate hyperthermia conditions [Vallez, Plourde, and Abraham, 2016] used experimental data to determine some parameters that can be used not only on the rewarming stage but also during the whole procedure of hypothermia using a cooling mattress.

In this work, the Pennes bioheat equation was used to simulate bioheat transfer in the human body, and the model that represents heat exchange on the circulatory system described in [Fiala, 1998] was implemented in a three-dimensional finite element code to simulate hypothermia treatments in adults. The in-house software was developed at the Structure and Materials Laboratory at the Federal University of Rio de Janeiro, as a continuation of the work of [Silva, 2012, 2016]. Numerical analyses of whole body cooling methods were performed to compare the efficacy of cooling mattress and intravascular catheter procedures during rapid cooling, maintenance of cooling and rewarming phase of the therapy. A thermoregulation model capable of simulating a real cooling therapy can be used to assist clinical trials for hypothermia techniques, simulating the best options to be used during treatment and improving low cost methods that could be used in hospitals and clinics that cannot afford expensive techniques.

2. Methodology

2.1. Bioheat Transfer

In this paper, the calculation of a whole body thermal analysis will be based on a blood perfusion continuum macro-scale bioheat model developed by Pennes [Bhowmik, Singh, Repaka, and Mishra, 2013]:

$$\rho_t c_t \frac{\partial T_t}{\partial t} = \nabla \cdot (k_t \nabla T_t) + \rho_b c_b \omega_b (T_a - T_t) + \dot{q}_m \tag{1}$$

and represents the bioheat flux in a domain Ω . The symbol T is the temperature and the subscripts t, b, a and m represent tissue, blood, arterial blood and metabolism, respectively. The material properties defined in the equation are: k (thermal conductivity), c (specific heat), ρ (density) and ω (blood perfusion rate). The metabolic heat generation rate is represented by $\dot{q}_m$. The values of the parameters will be defined in the next section.

For each tissue of the body are defined different properties. Prescribed temperatures $\overline{T}(\Gamma_t.t)$ in the boundary Γ_t and heat fluxes $\overline{q}(\Gamma_q, t)$ in the boundary

Γ_q are defined as boundary conditions in the boundary $\Gamma = \Gamma_t \cup \Gamma_q$. The initial condition is

$$T(x, t_0) = T_0, \tag{2}$$

where T_0 is the initial temperature in each tissue,which may vary according to the position within the body.

2.2. Metabolism

The metabolic heat generation rate in each tissue is composed of the basal rate $\dot{q}_{m,0}$, and an additional rate $\Delta\dot{q}_m$ generated by a local thermoregulation activity [Fiala, 1998]:

$$\dot{q}_m = \dot{q}_{m,0} + \Delta\dot{q}_m \tag{3}$$

The rate $\Delta\dot{q}_m$ is composed of three terms:

$$\Delta\dot{q}_m = \Delta\dot{q}_{m,0} + \Delta\dot{q}_{m,sh} + \Delta\dot{q}_{m,w} \tag{4}$$

where the local basal metabolic variation is $\Delta\dot{q}_{m,0}$ and variations due to changes in metabolism are represented by the terms $\Delta\dot{q}_{m,sh}$ and $\Delta\dot{q}_{m,w}$. These variations are caused by shivering and muscular effort, and occurs only in muscular tissues. The local basal metabolic variation can be calculated by [Fiala, Lomas, and Stohrer, 1999]:

$$\Delta\dot{q}_{m,0} = \dot{q}_{m,0}[Q_{10}^{\frac{T_t - T_0}{10}} - 1] \tag{5}$$

where T_0 is the temperature of thermal neutrality, equal to 30^oC and the Q_{10} coefficient is responsible for changes in the metabolic heat generation rate and blood perfusion rate due to changes in the temperature of the tissues, defined from experimental measurements to be in a range between 2 and 4 and usually considered as equal to 2 [Fiala, Havenith, Bröde, and B. Kampmann, 2012]. The shivering effect may be neglected because it may be controlled in a medical

procedure for adults. The muscular response may also be omitted since the hypothermia treatment does not involve muscular activities that may increase the metabolic heat generation at a significant level.

2.3. Arterial Temperature

In Eq. (1) the term that represents the blood perfusion considers that the heat exchange between blood and tissues occurs only on the capillary vessels, but adjacent arteries and veins exchange heat in the body extremities, where the blood is colder than in the core. These effects must be considered in the model, as the tissue temperature influences the arterial blood temperature. To take this effect into account the arterial temperature calculation is performed by a circulatory system model described in [Fiala, 1998, Silva, Laszczyk, Wrobel, Ribeiro, and Nowak, 2016].

This model assumes that the arterial temperature has different values in different regions of the human body, called sectors. The central sectors have an arterial temperature equal to the blood pool temperature while the arterial temperature of the extremities is influenced by the countercurrent heat exchange effect. Assuming mass continuity in blood vessels and the net flow rate from the equation of Gordon [Gordon, 2001], the arterial temperature can be calculated as:

$$T_a = \frac{\dot{m}_b \, c_b T_p + h_x T_v}{\dot{m}_b \, c_b + h_x} \tag{6}$$

In the above equation, T_p is the blood pool temperature, T_a and T_v are the arterial and venous temperatures and h_x is the counter current heat exchange coefficient, considered as zero in the core and with defined values obtained from experimental measurements for the extremities of the body [Fiala, Lomas, and Stohrer, 1999].

As the bioheat equation assumes capillary blood is in equilibrium with the surrounding tissue[Fiala, 1998], the calculation of T_v in a body element can be

obtained as follows:

$$T_{v_{element}} = \frac{\int \omega_b \, T_t \, dV}{\int \omega_b \, dV} \tag{7}$$

This means the venous blood leaving the body element is equal to the local tissue temperature of the element.

The implementation presented here is similar to the model applied for neonates described in [Laszczyk and Nowak, 2015a, Silva, Laszczyk, Wrobel, Ribeiro, and Nowak, 2016], and is a fully continuum three-dimensional model that considers that all sectors of the body are connected and all surfaces exchange heat. The numerical procedure to calculate T_a, T_v and T_p will be shown in Section 2.7.

2.4. Blood Perfusion Rate

The blood perfusion rate $\omega_{b,t}$ in a specific tissue can be described as a composition of two terms:

$$\omega_{b,t} = \omega_{b,0,t} + \Delta\omega_{b,t} \tag{8}$$

where $\omega_{b,0,t}$ stands for the local basal blood perfusion rate and $\Delta\omega_{b,t}$ is a local temperature-dependent variation. Assuming that the local blood perfusion rate is coupled with the local metabolic heat generation [Diao, Zhu, and Wang, 2003], this local variation may be calculated as:

$$\Delta\omega_{b,t} = \omega_{b,0,t}\left[Q_{10}^{\frac{T_t - T_0}{10}} - 1\right] \tag{9}$$

Similarly to Eq.(5), the reference temperature T_0 is the temperature of thermal neutrality and the Q_{10} coefficient is usually considered as equal to 2.

2.5. External Heat Exchange

The external heat exchange is sum of the contributions of three main mechanisms: convection, radiation and evaporation. The heat exchange rate varies

along the body surface, and the heat flux consists of the convective, radiative and evaporative fluxes:

$$q_{skin} = q_{conv} + q_{rad} + q_{evap} \tag{10}$$

The convective flux q_{conv} between the environment and the body boundaries consists of the skin surface and it can be obtained using the Newton cooling law, defined as

$$q_{conv} = h_{conv} \, . \, (T_{ext} - T_{skin}) \tag{11}$$

The symbol T_{ext} represents the external air temperature and h_{conv} is the convective heat transfer coefficient.

The radiative flux is calculated using the Stefan-Boltzmann law:

$$q_{rad} = h_{rad}(T^4_{skin} - T^4_{sr,mean}) \tag{12}$$

where T_{skin}, $T_{sr,mean}$ and h_{rad} are the temperatures at the skin surface, the temperature of the radiation source on the exterior of the domain, and a radiative parameter, respectively, and

$$h_{rad} = \sigma \, \varepsilon \tag{13}$$

in which σ refers to the Stefan-Boltzmann constant and ε is the emissivity of the external skin surface. The value of the emissivity varies according to the surface material.

The evaporative flux was incorporated in the model as a prescribed heat flux boundary condition to consider heat losses by evaporation, based on values described in the literature. In the applications described in this paper the basal evaporation rate from the skin was considered as $18W$ (taken from [Fiala, Havenith, Bröde, and B. Kampmann, 2012]).

Respiration losses were incorporated on the material thermal properties of the trunk/head sectors, as respiration can be responsible for a loss of 25% of whole-body metabolic heating [Vallez, Plourde, and Abraham, 2016].

The value of the external heat transfer coefficient may be adjusted to simulate clothed or unclothed situations as discussed in [Al-Othmani, Ghaddar, and Ghali, 2008].

2.6. Lumped Analysis for Blood Cooling

One of the most effective ways to reduce body temperature is to use intravascular cooling catheters that directly cool the major veins and can achieve cooling rates of $5.0^oC/hour$ depending on the capacity of the device [Dae, Gao, Ursell, Stillson, and Sessler, 2003]. In these procedures, the blood temperature is actively lowered or increased. The simulation of blood cooling for hypothermia treatments using methods applied directly to the blood vessels, as intravenous saline fluid infusion or an intravascular catheter, needs an additional equation coupled to the Pennes bioheat equation to account for the tissue-blood thermal interactions.

The model implemented in this paper considers the energy balance of a blood compartment as a lumped system that combines the energy added or subtracted by an external device and the loss of heat from blood to tissues during circulation. This model, adapted from [Zhu, Schappeler, Cordero-Tumangday, and Rosengart, 2009], provides a method to obtain blood and body temperatures during active blood temperature modifications and is capable of simulating the stages of cooling and rewarming of blood during hypothermia procedures to treat strokes and brain damages in adults.

The mathematical model consists of a coupled simulation of body temperature distribution and blood energy balance, and couples the Pennes bioheat equation (Eq. 1) and an equation of energy balance of the blood compartment of the body to predict blood temperature change during clinical aplications. Because of the relatively short recalculation time, blood in the human body is represented as a lumped system. The governing equation for the blood temperature can be written as [Zhu, Schappeler, Cordero-Tumangday, and Rosengart,

2009]

$$\rho_b c_b V_b \frac{dT_a}{dt} = Q_{ext}(T_a, t) - Q_{b-t}(t) = Q_{ext}(T_a, t) - \rho_b c_b \overline{\omega} V_{body}(T_a - \overline{T_t}) \quad (14)$$

where Q_{ext} represents the capacity of the external device and can be a function of arterial temperature or time, and V_{body} stands for the volume of the body. The parameter $\overline{\omega}$ is the mean volumetric blood perfusion rate, calculated by:

$$\overline{\omega} = \frac{1}{V_{body}} \iiint_{V_{body}} \omega dV_{body} \quad (15)$$

and $\overline{T_t}$ is the weight-average tissue temperature, defined by the relation:

$$\rho c \omega (T_{a0} - \overline{T_t}) V_{body} = \iiint_{V_{body}} \rho c \omega (T_{a0} - T_{t0}) dV_{body} \quad (16)$$

where T_{a0} stands for the arterial temperature before time step $t + \Delta t$ and T_{t0} represents the tissue temperature before time step $t + \Delta t$. At steady-state, the arterial temperature T_a should be the same as the weight-average tissue temperature $\overline{T_t}$.

The numerical procedure for the implementation of this model will be shown in the next section.

2.7. Numerical Model

The solution of the Pennes bioheat equation and the circulatory model described in section 2.4 is obtained using the finite element method The transient problem is solved using a time-marching scheme based on a semi-discrete form of the finite element method (FEM). The numerical model is described in [Silva, Laszczyk, Wrobel, Ribeiro, and Nowak, 2016]. Considering Eq. (1) in a spatial domain Ω and a temporal interval $(0, \Pi)$, the domain Ω is discretized into elements and at each time step $t = t_{n+1}$, the following system of algebraic equations is obtained:

$$M\,\dot{T}_{n+1} + K\,T_{n+1} = F_{n+1} \quad (17)$$

where M is the mass matrix, $\dot{T}_{n+1}$ stands for the nodal values of the time derivative of temperature, K is the stiffness matrix, T_{n+1} are the nodal temperatures at time step t_{n+1} and F_{n+1} is the vector of independent terms. The coefficients of these matrices are calculated as follows:

$$m_{ij} = \int_{\Omega} c_t \rho_t N_i N_j d\Omega \tag{18}$$

$$K_{ij} = k_t \int_{\Omega} (\frac{\partial N_i}{\partial x}\frac{\partial N_j}{\partial x} + \frac{\partial N_i}{\partial y}\frac{\partial N_j}{\partial y} + \frac{\partial N_i}{\partial z}\frac{\partial N_j}{\partial z}) d\Omega + \int_{\Omega} c_b \rho_b \omega_b N_i N_j d\Omega \tag{19}$$

$$f_i = \int_{\Omega} \dot{q}_m N_i d\Omega - \int_{\Gamma} \overline{q} N_i d\Gamma + \int_{\Omega} c_b \rho_b \omega_b T_a N_i d\Omega \tag{20}$$

The counter current heat exchange effect and the changes in arterial temperature are calculated for each sector $T_{a,l}$ as

$$T_{a,l} = \frac{\rho_b \, c_b \Big(\sum_{i=1}^{N_l} \omega_{b,t,l} \, V_{i,t,l} \Big) \; T_p + h_{x,l} T_{v,l}}{\rho_b \, c_b \Big(\sum_{i=1}^{N_l} \omega_{b,t,l} \, V_{i,t,l} \Big) + h_{x,l}} \tag{21}$$

where the subscript l denotes the sector of the body, the number of elements in each sector l is denoted by N_l and the volume of element i of the tissue t in the sector l is $V_{i,t,l}$.

As the venous temperature of each element is equal to the tissue temperature, to calculate the venous temperature $T_{v,l}$ in each sector, Eq. (7) can be incorporated to the numerical model as:

$$T_{v,l} = \frac{\rho_b \, c_b \Big(\sum_{i=1}^{N_l} \omega_{b,t,k} \, V_{i,t,l} T_{i,t,l} \Big)}{\rho_b \, c_b \Big(\sum_{i=1}^{N_l} \omega_{b,t,l} \, V_{i,t,l} \Big)} \tag{22}$$

The blood pool temperature can be written as:

$$T_p = \frac{\sum_{l=1}^{L}\Big[\dfrac{\rho_b\, c_b\Big(\sum_{i=1}^{N_l}\omega_{b,t,l}\, V_{i,t,l}\Big)\;\; \rho_b\, c_b\Big(\sum_{i=1}^{N_l}\omega_{b,t,l}\, V_{i,t,l}\, T_{i,t,l}\Big)}{\rho_b\, c_b\Big(\sum_{i=1}^{N_l}\omega_{b,t,l}\, V_{i,t,l}\Big) + h_{x,l}}\Big]}{\sum_{l=1}^{L}\Big[\dfrac{\Big[\rho_b\, c_b\Big(\sum_{i=1}^{N_l}\omega_{b,t,l}\, V_{i,t,l}\Big)\Big]^2}{\rho_b\, c_b\Big(\sum_{i=1}^{N_l}\omega_{b,t,l}\, V_{i,t,l}\Big) + h_{x,l}}\Big]} \tag{23}$$

where L is the total number of sectors in the body and $T_{i,t,l}$ is the temperature of each element i of tissue t in sector l. For the treatment of the non-linearities a predictor multi-corrector algorithm was used [Hughes, 1987], as described in [Silva, Laszczyk, Wrobel, Ribeiro, and Nowak, 2016].

For the method described in section 2.7 for blood cooling applications in adults, the transient problem represented by Eq. (14) can be discretized by finite differences. The implicit discretization scheme results in the calculation of the arterial temperature as:

$$T_a^{n+1} = \frac{\frac{Q_{ext}\Delta t}{\rho_b c_b V_b} + T_a^n + \overline{T_t^n}\,(\frac{\rho_b c_b \overline{\omega} V_{body}\Delta t}{\rho_b c_b V_b})}{1 + \frac{\rho_b c_b \overline{\omega} V_{body}\Delta t}{\rho_b c_b V_b}} \tag{24}$$

In this case, the same iterative solver and element calculation procedures of the previous model is used. The calculation of the temperature T_a^{n+1} is performed before step 5 at each new time step.

3. Applications

The geometrical model used for simulations of adults was obtained by segmentation of 3D medical images (CT scans) of the Visible Human Data Set (VHD) provided by the National Library of Medicine, US Department of Health and Human Services. The medical images were used to generate the geometry using the software *MIMICS* and adapted using the packages *ANSYS Workbench*

and *Trelis* to generate a 13 million mesh of a male adult with a body weight of $100kg$, body surface area of $2.27m^2$, $1.88m$ height, a cardiac output of $6l/min$ and 28% body fat content. The total basal whole body metabolism is $106W$ and basal evaporation rate from the skin of $18W$ (taken from [Fiala, Havenith, Bröde, and B. Kampmann, 2012]). The simulations were performed using a platform comprised by two Xeon $E5-5420$ processors with $64GB$ of RAM and 12 cores.

The geometry of the body is composed of eight different materials: skin+fat, muscle, bone, brain, viscera, lungs, eyes and cerebrospinal fluid). For the calculation of the arterial temperature, the body is divided in six sectors: trunk + abdomen, head, arm, hand, leg, foot. The simulations where performed in a geometry of half of the body, due to symmetry. The materials and division into sectors are depicted in Figures 1-4.

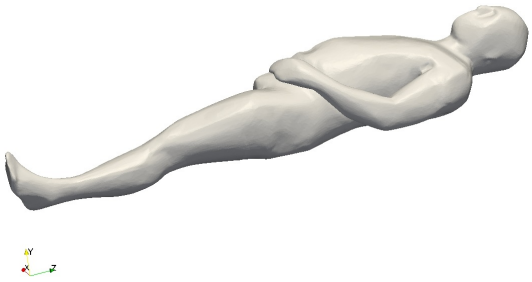

Figure 1: Geometry of the male adult

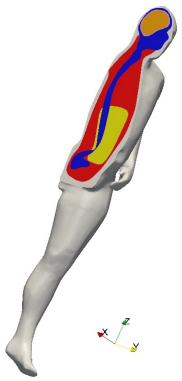

Figure 2: Geometry of the male adult, internal organs

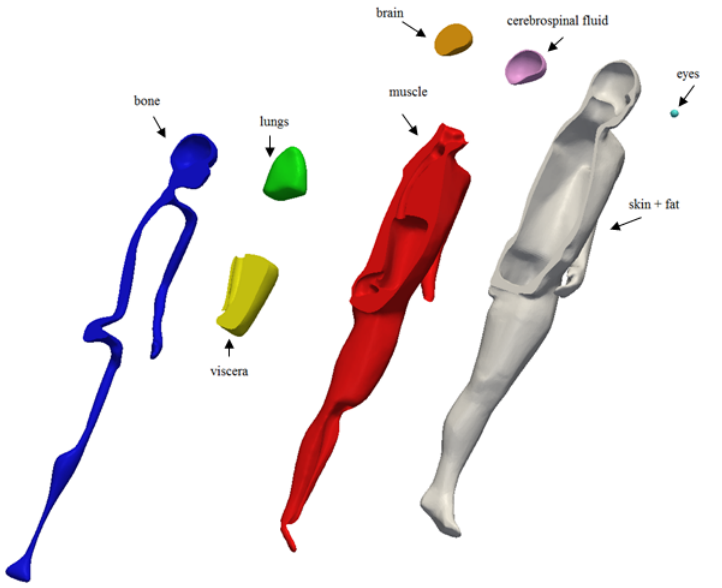

Figure 3: Geometry of the tissues

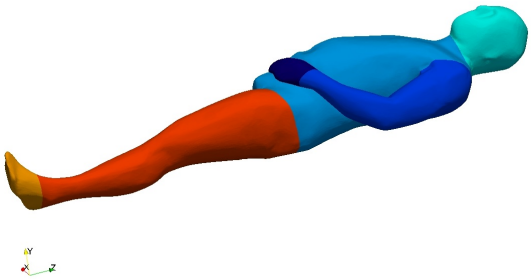

Figure 4: Division into sectors

The finite element mesh consisted of 13 million four-node tetrahedral elements. A zoom in the upper region of the body is shown in Figure 5.

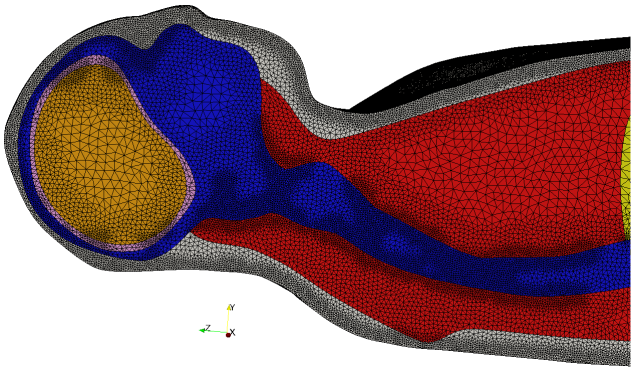

Figure 5: Zoom -Mesh of 13.0 million elements

The thermophysiological properties of the human tissues were taken from the literature, adapted from [Vallez, Plourde, and Abraham, 2016, Fiala, 1998, Hasgall, Gennaro, Baumgartner, Neufeld, Gosselin, Payne, Klingenbock, and Kuster, 2015]. Table 1 shows the tissue thermophysiological properties used in this simulation. Metabolic heat generation rates used in the simulation consider the impact of respiration on heat loss corresponding to 25% of the whole-body metabolic heating [Vallez, Plourde, and Abraham, 2016], distributed over the elements belonging to the sectors trunk+abdomen and head. The counter current heat exchange coefficients were taken from [Fiala, 1998] and are presented in Table 2.

Table 1: Thermophysiological properties of the different tissues

Material properties					
Tissue	Thermal Conductivity ($W/m.^oC$)	Density (kg/m^3)	Specific Heat ($J/kg.^oC$)	Metabolic Heat Generation Rate (W/m^3)	Blood Perfusion Rate ($1/s$)
Blood	0.5	1050	3800	-	-
Eye	0.43	1076	4200	0	0
Lungs	0.39	394	3886	1835	0.0008677
Skin + Fat	0.2	877	2727	170	0.0003146
Cerebrospinal fluid	0.57	1007	380	0	0
Bones	1.16	1300	1590	0	0
Muscle	0.5	1050	3770	528	0.0005355
Viscera	0.55	1100	3350	3160	0.004532
Brain	0.53	1360	2450	12954	0.013124

Table 2: Counter current heat exchange coefficient of the seven sectors of the body

Countercurrent heat exchange coefficient - h_{xc} ($W/^oC$)						
Sector	Head	Trunk+Abdomen	Arm	Hand	Leg	Foot
	0.000	0.000	4.13	0.57	6.2	1.45

312 The first example used to validate the adult geometry and tissue properties
313 in these simulations was taken from [Vallez, Plourde, and Abraham, 2016, Fiala,
314 Lomas, and Stohrer, 1999] and consists of a male human in an environment in
315 thermal neutrality. The boundary conditions consist of a convective heat flux at

the skin surface (Eq.11). The skin surface was exposed to a room temperature of 30^oC and a heat transfer coefficient value of $7W/m^2.^oC$ was used, as defined in [Vallez, Plourde, and Abraham, 2016, Fiala, Lomas, and Stohrer, 1999].

The simulation of the WBC procedure was based on temperature results found in different clinical studies [Wang, Olivero, Lanzino, Elkins, Rose, and Honings, 2004, Yang, Ou, and Chen, 2006, Harris, Muh, Surles, Pan, Rozycki, and Macleod, 2009, Callaway, Tadler, Katz, Lipinski, and Brader, 2002] and the boundary conditions of the numerical simulations [Fiala, 1998, Vallez, Plourde, and Abraham, 2016, Laszczyk and Nowak, 2015a] were considered to perform analyses that match the same values obtained in the clinical trials. The target was to reduce core temperature to around 34^oC after $1-4$ hours, maintaining the temperature at this level during 24 hours and then rewarming the body at a rate of $0.15-1.45^oC/hour$. Although the body temperature can be higher or lower than the normal temperature depending on the trauma, the examples presented in this work consider an initial body temperature of 37^oC.

Whole body cooling simulations were performed considering a cooling mattress on the bottom part of the body, where convective heat fluxes were prescribed using Eq. 11, and heat transfer to the room environment on the top part, with convective heat fluxes prescribed using Eq. 11. Evaporative heat fluxes were also considered on the top part of the body as a prescribed heat flux, calculated using the basal evaporation rate from the skin. For the top part, the total heat flux at the skin surface is composed by the sum of convective and evaporative heat fluxes:

$$q_{skin} = q_{conv} + q_{evap} \tag{25}$$

and the evaporative heat flux q_{evap} can be calculated according to

$$q_{evap} = \frac{Q_{evap}}{A_{top}} \tag{26}$$

where Q_{evap} represents the basal evaporation rate and A_{top} the area of the top surface of the body. The flux per unit of area was given at each external bound-

ary surface element to calculate the equivalent nodal loads. Both boundary regions are depicted in Fig. 6.

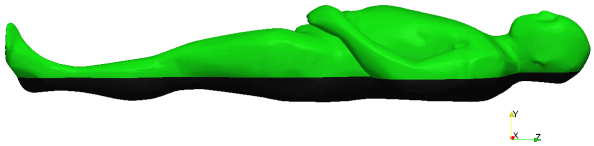

Figure 6: Top (green) and bottom (black) surfaces used to prescribe boundary conditions in whole body cooling

For the top surface, a room temperature of 25^oC was prescribed and a convective heat transfer coefficient of $7W/m^2.^oC$ is used. The contact between body and cooling mattress is simulated by a convective flux prescribed at the bottom surface, considering an initial temperature of 10^oC during the first 2 hours of analysis. After this initial rapid cooling, the cooling mattress temperature is set to 33^oC during 22 hours. The convective heat transfer coefficient was set to $10W/m^2.^oC$, based on experimental studies found in [Vallez, Plourde, and Abraham, 2016]. A second subcase was performed considering a room temperature of 20^oC and comparing the results. After 2 hours of simulation the cooling mattress temperature has been set to 34^oC during the rest of the analysis.

The third example demonstrates the validity of our model for transient conditions. It consists of the simulation of the rewarming phase using the same boundary conditions of the cooling mattress case during 24 hours and then raising the temperature of the mattress. The mattress temperature was set to different values to compare core temperature behaviour. In this case, mattress temperatures of 37^oC, 42^oC and 45^oC were used.

Test four demonstrates the viability of cooling using an intravascular catheter, with a novel numerical method adapted from [Zhu, Schappeler, Cordero-Tumangday, and Rosengart, 2009], which is used for the first time in a comprehensive whole body cooling model. For this case, the same boundary regions (top and bottom) of the previous case are used. The mattress in this case does not exchange heat and is considered as an insulated surface during the first hour of simula-

tion(prescribed heat fluxes at the bottom part are null). After the first hour, the mattress temperature is set to 33^oC and the heat transfer coefficient of $10W/m^2.^oC$ is used (Eq.11). The top surface is subject to a convective flux with a heat transfer coefficient of $7W/m^2.^oC$ (Eq. 11) and a prescribed evaporative heat flux based on the basal evaporation rate from the skin.. The heat exchanged by the device is $100W$ during the first hour of simulation; after this period, the device is turned off. The idea is to use the device for rapid cooling and then maintain the temperature at a hypothermia level using a cooling mattress.

4. Results

In the first case, conditions of thermal neutrality were imposed and a transient simulation was performed until a steady-state solution was obtained. The core temperature was defined as equal to the blood pool temperature calculated during the simulation. The core temperature was extracted and compared to normothermic values of a human subject to a 30^oC room temperature. The results showed a core temperature of 37^oC, in agreement with values from other studies [Vallez, Plourde, and Abraham, 2016, Fiala, 1998]. The mean skin surface temperature was 34.3^oC, consistent with the results of published data for neutrality conditions described by [Fiala, 1998], where the mean skin surface temperature of 34.4^oC has been obtained.

The second case analyses core temperature during a whole body cooling treatment using a cooling mattress. Figure 7 shows changes in blood pool temperature during the 24 hour procedure.

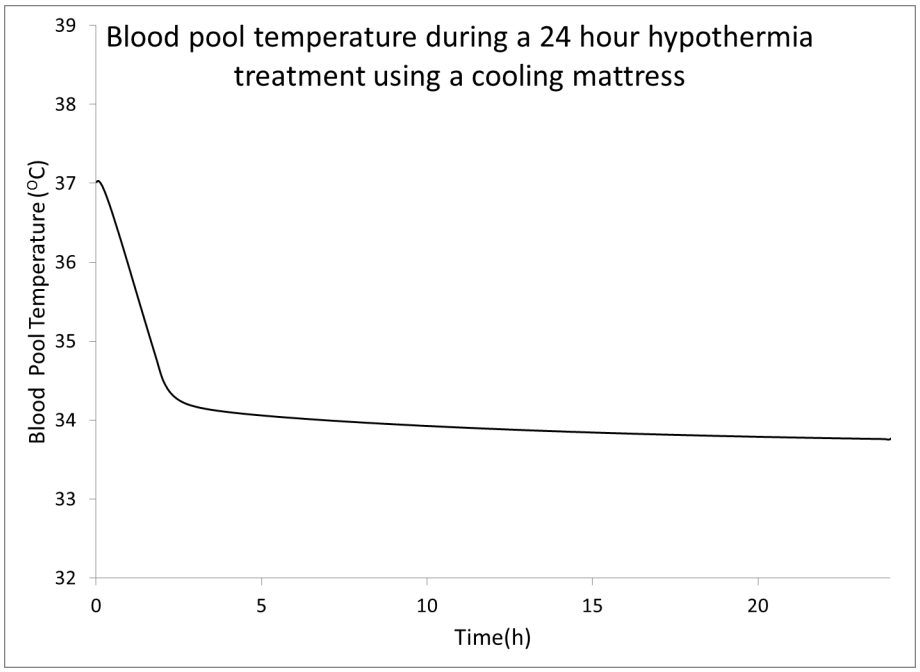

Figure 7: Second case: Core temperature during a 24 hour treatment using a cooling mattress.

The results show a drop in the blood pool temperature to 34^oC after 2 hours of simulation and the core temperature reaches the minimum value of 33.8^oC at the end of the simulation. The temperature profile at the end of the analysis at the outer skin and internal organs is depicted in Fig. 8 and Fig. 9. It should be noted that the interface between the upper and bottom boundary conditions is a continuons field, not a step function as may be misinterpreted from Fig. 8

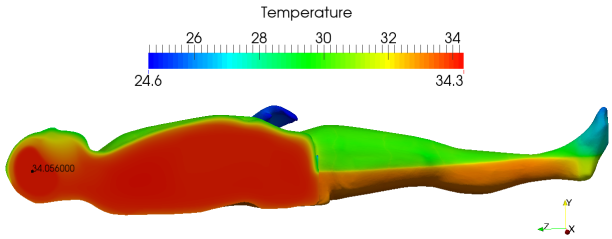

Figure 8: Second case: Internal temperature distribution after a 24 hour treatment.

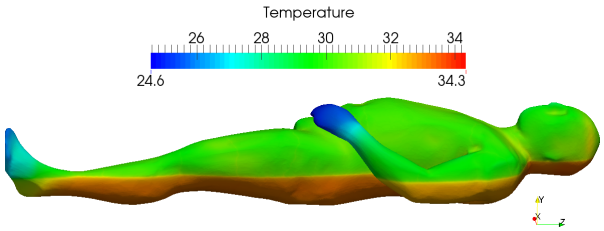

Figure 9: Second case: Skin temperature distribution after a 24 hour treatment.

The temperature profile shows a minimum brain temperature of 34.1^oC at the end of the simulation. The temperature distribution at the top skin surface has a range between $24.6 - 30^oC$, and the minimum values are found in the extremities (hands and feet).

The third case analyzes core temperature during the rewarming phase of the WBC treatment. Three analyses were performed, considering the mattress temperature set to 37^oC, 42^oC and 45^oC. Figure 10 shows a comparison between the blood pool temperature during 7 hours of rewarming for the three cases analyzed.

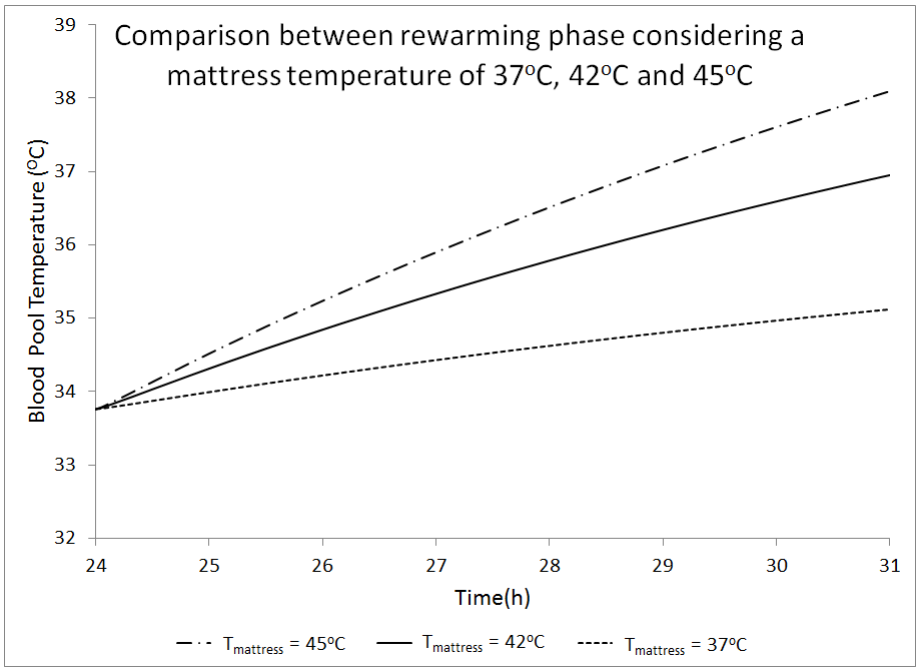

Figure 10: Third case: Comparison between core temperature after a 24 hour hypothermia treatment using different mattress temperatures.

The results show a considerable influence of the mattress temperature in the core temperature during the rewarming phase. The fastest rewarming rate is $0.63^oC/hour$, for the mattress temperature of 45^oC. Rewarming rates of $0.47^oC/hour$ and $0.20^oC/hour$ were obtained for mattress temperatures of 42^oC and 37^oC, respectively. Based on these results, the more suitable rewarming mattress temperature for a real case is 42^oC. The core temperature during the whole simulation (rapid cooling, cooling and rewarming) for the 42^oC rewarming mattress temperature is shown in Fig. 11.

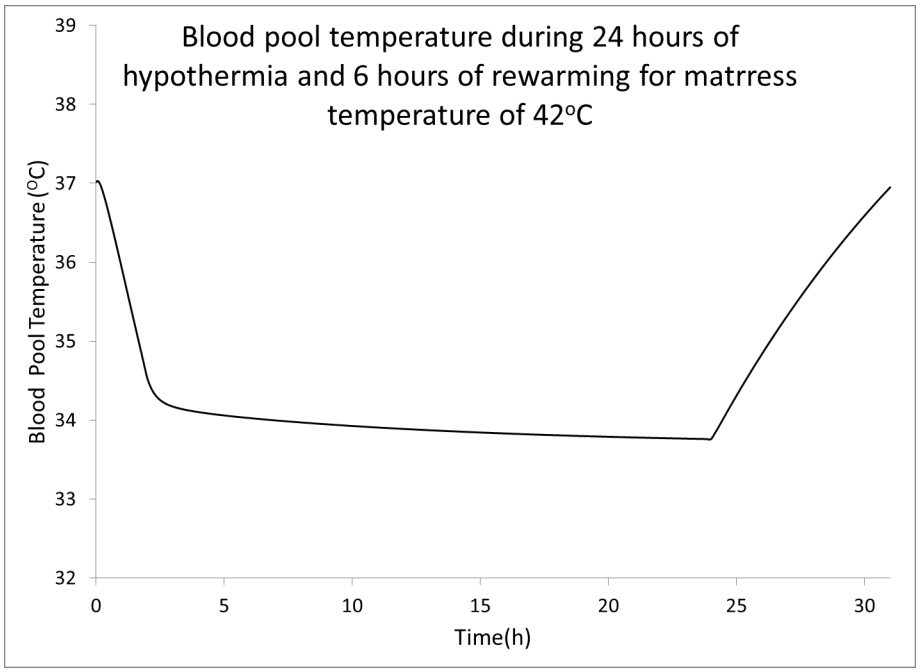

Figure 11: Third case: Core temperature during 24 hours of hypothermia and 6 hours of rewarming for mattress temperature of 42.0^oC.

412 The temperature profile at the end of the analysis at the outer skin and
413 internal organs is depicted in Fig 12 and Fig. 13.

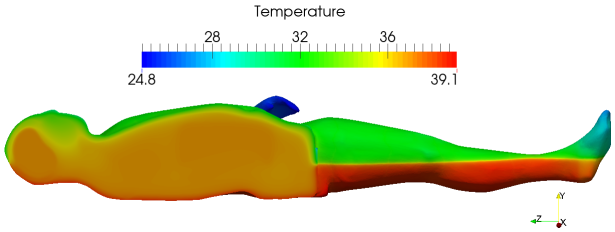

Figure 12: Third case: Internal temperature distribution after rewarming.

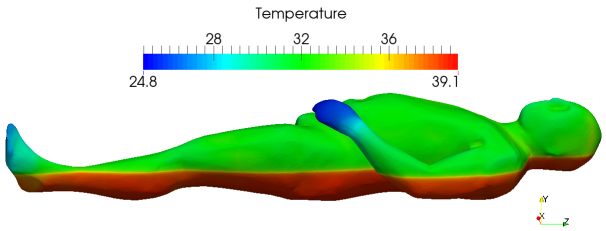

Figure 13: Third case: Skin temperature distribution after rewarming.

The temperature profile shows the brain temperature reestablishes the normothermic value at the end of the simulation. The temperature distribution at the top skin surface has a range between $24.8 - 32^oC$, and the minimum values are found in the extremities (hands and feet).

A second simulation using the same parameters and a room external temperature of 20^oC is performed to compare the behaviour and distribution of temperatures for a decrease in the room temperature of 5^oC. The comparison between core temperature during rapid cooling, cooling maintenance and rewarming is plotted in Fig. 14.

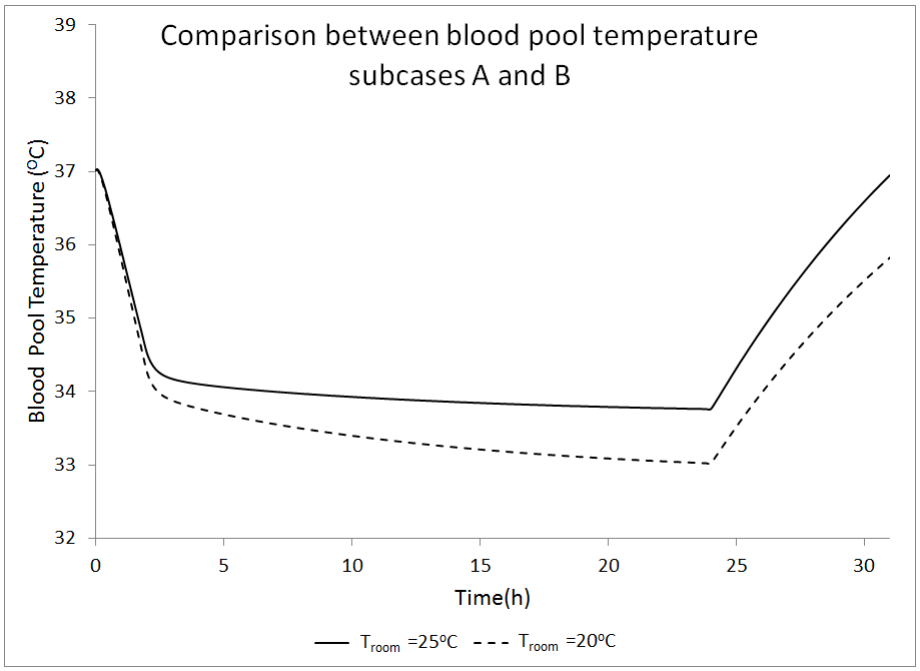

Figure 14: Third case: Comparison between core temperature during 24 hours of hypothermia and 6 hours of rewarming for mattress temperature of 42.0^oC for room temperature of 25.0^oC and 20.0^oC.

The above figure shows a decrease of 5^oC in the room temperature reduces the minimum value of the core temperature to 33^oC after a 24 hour treatment. The rewarming rate for subcase B is $0.42^oC/hour$, 8.5% lower than the original case for external temperature of 25^oC.

The fourth case considers the anatomical geometry shown in Figure 1 for direct blood cooling. The simulation of an invasive procedure using an intravascular catheter uses an insulated mattress during the first hour of simulation and a room temperature of 25^oC. The blood cooling procedure is treated as an external device with capacity of $100W$ applied during the first hour of simulation. After the first hour, the mattress temperature is set to 33^oC with a heat transfer coefficient of $10W/m^2.^oC$ and the intravascular catheter is turned off. Results of arterial temperature during 24 hours are shown in Fig. 15.

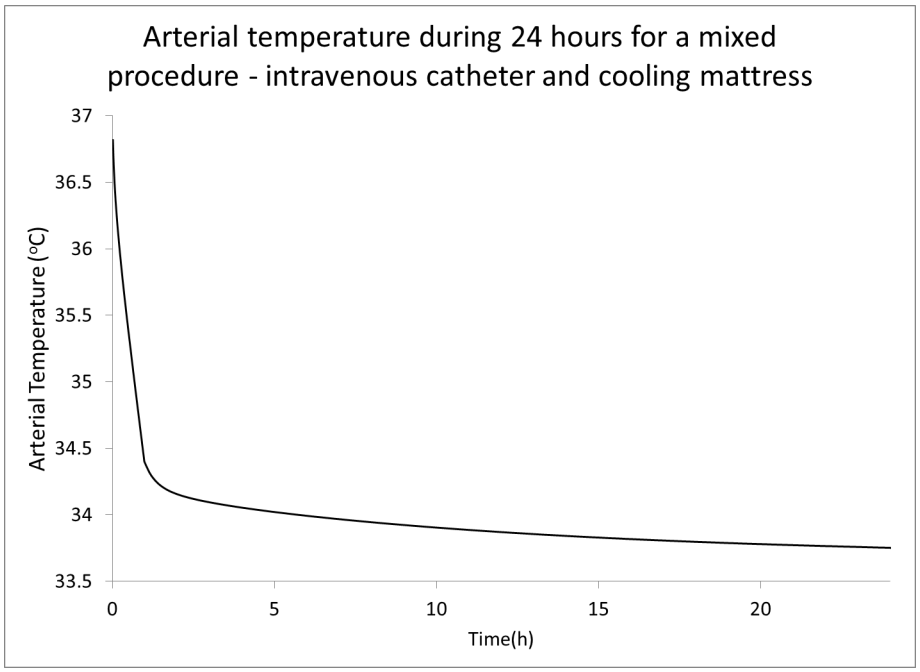

Figure 15: Fourth case: Arterial temperature during 24 hours of a mixed hypothermia procedure - intravenous catheter and cooling mattress.

The results show a drop in arterial temperature of 2.6^oC during the first hour of simulation. After this period, the cooling rate is reduced and the temperature drops from 34.4^oC to 33.6^oC during the next 23 hours of simulation.

5. Conclusion

The main goal of the work described in this paper was to develop a finite element model able to simulate bioheat transfer processes in adults, and to perform whole body cooling procedures as a treatment for brain traumas. The Pennes bioheat model was chosen to simulate the bioheat transfer processes in a macroscale and the blood pool approach described in [Fiala, 1998] was considered to take into account changes in the arterial temperature due to the circulatory system and heat transfer with the environment. For blood cool-

ing using an intravenous catheter, a blood cooling approach described in [Zhu, Schappeler, Cordero-Tumangday, and Rosengart, 2009] was used.

The whole body cooling method applied to the adult body produced satisfactory results in reducing brain/core temperature to less than 34^oC in two hours. The moderate hypothermia was maintained for 22 hours with a core temperature around $34.0 - 33.8^oC$. As stated previously, the brain temperature remained $0.2 - 0.3^oC$ above/below core temperature during the whole analysis. The mattress had to be set to a temperature of 42^oC to allow a smooth increase of core temperature, at a rate around $0.5^oC/hour$. Although this value is defined as the ideal rewarming rate, [Wang, Olivero, Lanzino, Elkins, Rose, and Honings, 2004] reported values of $0.15 - 1.45^oC/hour$ measured on randomised trials, showing that the rewarming procedures are not always able to maintain cooling rates close to the ideal value.

The blood cooling simulation, considering an intravascular catheter, was able to reduce core temperature to less than 34^oC in one hour. After the intravascular catheter was removed, the cooling mattress was set to a temperature of 33^oC. The mixed method was able to simulate a hypothermia treatment with rapid cooling and maintenance of cooling at moderate hypothermia levels during 24 hours. Suggestions of a study using mixed methods, considering head cooling methods to maintain cooling after induction of hypothermia with cold intravenous fluids were mentioned in [Harris, Andrews, Murray, Forbes, and Moseley, 2012], but no results were found in clinical trials mixing blood cooling with WBC methods.

The results of different cooling methods demonstrate the importance of the developed model for the study of different cooling procedures. The simulations presented in this work reproduce a hypothermic treatment in a realistic adult body with results similar to values reported in the literature [Harris, Andrews, Murray, Forbes, and Moseley, 2012, Hoque, Chakkarapani, Liu, and Thoresen, 2010, Unit, 2006]. This opens the way for the optimization of the treatment on a patient-specific basis.

The major limitations in the use of this type of model are associated with

the correct definition of the geometry and the input parameters, very important to obtain good results. In the cases discussed here, the FEM mesh was generated based on a geometry obtained from CT scans, so the model for the human body is based on a real geometry. One of the greatest difficulties of the numerical model is the determination of the correct parameters to guarantee that the analysis corresponds to the real case, as small differences in some of the parameters can result in substantial differences in temperature, as demonstrated by the sensitivity analysis in [Silva, Laszczyk, Wrobel, Ribeiro, and Nowak, 2016]. A sensitivity analysis performed for a neonate model [Silva, Laszczyk, Wrobel, Ribeiro, and Nowak, 2016] shows the importance of correctly determining input parameters as external temperature and heat transfer coefficient. For the correct determination of parameters, at this stage of the research literature values were used, adapted from other numerical simulations [Vallez, Plourde, and Abraham, 2016, Fiala, 1998] and from an experimental database source [Hasgall, Gennaro, Baumgartner, Neufeld, Gosselin, Payne, Klingenbock, and Kuster, 2015].

Calibration of the model using real hypothermia cases could be used as a starting point to test cost-effective methods for brain/body cooling. Experiments for determination of the convective heat transfer coefficient should be conducted to establish a standard database for bioheat transfer in the human body. After validation, tests of cost-effective methods could be used as a standard protocol in clinics and hospitals for public health care, reducing neurological damages after cerebral traumas.

Although the benefits of hypothermia for post-traumatic brain injuries in adults is widely known, the uncertainties about effectiveness and robust evidence of reducing brain temperature during clinical trials makes it difficult to define a cooling method to be used for each case of trauma. Whole body cooling is a promising method that still needs further research and more robust evidence of temperature reduction. Studies should describe clear baseline temperatures, duration of cooling, temperatures achieved and temperature changes with cooling, along with side effects of each method. In this way, joint research between engineers and clinicians could fill some empty spaces and collaborate to reduce

post-traumatic neurological damage in patients suffering brain traumas.

Although the development of this three-dimensional finite element model was conducted with the objective of investigating hypothermia treatments, it can also be adapted to predict body temperature changes during exercises and different heat exposures. The numerical tool presented here can be improved and many additional time or temperature-dependent parameters can be added to simulate transient body temperature on different applications.

Acknowledgements: We thank the Carlos Chagas Filho Research Foundation of the State of Rio de Janeiro (FAPERJ) and the Coordination for the Improvement of Higher Education Personnel (CAPES), both in Brazil, for the financial support.

Conflicts of Interest: None

Funding: Carlos Chagas Filho Research Foundation of the State of Rio de Janeiro (FAPERJ) and the Coordination for the Improvement of Higher Education Personnel (CAPES)

Ethical Approval: Not required

References

M. Al-Othmani, N. Ghaddar, and K. Ghali. A multi-segmented human bioheat model for transient and asymmetric radiative environments. *International Journal of Heat and Mass Transfer*, 51:5522–5533, 2008.

A. Bhowmik, R. Singh, R. Repaka, and S.C. Mishra. Conventional and newly developed bioheat transport models in vascularized tissues: A review. *Journal of Thermal Biology*, 38(3):107–125, 2013.

C.W. Callaway, S.C. Tadler, L.M. Katz, C¿L. Lipinski, and E. Brader. Feasibility of external cranial cooling during out-of-hospital cardiac arrest. *Resuscitation*, 52:159–165, 2002.

M. Christiansen, N. Rakhilin, A. Tarakanova, and K. Wong. Modeling brain cooling treatment approved for hypoxic-ischemic encephalopathy in infants to treat stroke and cardiac arrest in adult patients. Cornell University, 2010.

M. W. Dae, D. W Gao, P. C. Ursell, C. A. Stillson, and D. I. Sessler. Safety and efficacy of endovascular cooling and rewarming for induction and reversal of hypothermia in human-sized pigs. *Stroke*, 34:734–738, 2003.

B. H. Dennis, R. C. Eberhart, G. S. Dulikravich, and S. W. Radons. Finite-element simulation of cooling of realistic 3-d human head and neck. *Journal of Biomechanical Engineering*, 125(6):832–840, 2003.

C. Diao, L. Zhu, and H. Wang. Cooling and rewarming for brain ischemia or injury: Theoretical analysis. *Annals of Biomedical Engineering*, 31(3):346–353, 2003.

D. J. Eicher, C. L. Wagner, L. P. Katikaneni, T. C. Hulsey, W. T. Bass, D. A. Kaufman, M. J. Horgan, S. Languani, J. J. Bhatia, L. M. Givelichian, K. Sankaran, and J. Y. Yager. Moderate hypothermia in neonatal encephalopathy: efficacy outcomes. *Pediatric Neurology*, 32:11–17, 2005.

D. Fiala. *Dynamic simulation of human heat transfer and thermal comfort*. PhD thesis, De Montfort University, Leicester, UK, 1998.

D. Fiala, K. J. Lomas, and M. Stohrer. A computer model of human thermoregulation for a wide range of environmental conditions: the passive system. *Journal of Applied Physiology*, 87(5):1957–1972, 1999.

D. Fiala, G. Havenith, P. Bröde, and G. Jendritzky B. Kampmann. UTCI-fiala multi-node model of human heat transfer and temperature regulation. *International Journal of Biometeorology*, 56(3):429–441, 2012.

C. J. Gordon. The therapeutic potential of regulated hypothermia. *Emergency Medicine Journal*, 18(2):81–89, 2001.

561 B. Harris, P.J.D. Andrews, G.D. Murray, J. Forbes, and O. Moseley. Systematic
562 review of head cooling in adults after traumatic brain injury and stroke. *Health*
563 *Technology Assessment*, 16(45):1–175, 2012.

564 O.A. Harris, C.R. Muh, M.C. Surles, Y. Pan, G. Rozycki, and J. Macleod.
565 Discrete cerebral hypothermia in the management of traumatic brain injury:
566 a randomized controlled trial. *Journal of Neurosurgery*, 110(6):1256–1264,
567 2009.

568 P. A. Hasgall, F. Di Gennaro, C. Baumgartner, E. Neufeld, M. C. Gosselin,
569 D. Payne, A. Klingenbock, and N. Kuster. IT'IS database for thermal and
570 electromagnetic parameters of biological tissues. Virtual Population Group,
571 2015.

572 R. W. Hickey and M. J.Painter. Brain injury from cardiac arrest in children.
573 *Neurologic Clinics*, 24:147–158, 2006.

574 N. Hoque, E. Chakkarapani, X. Liu, and M. Thoresen. A comparison of cooling
575 methods used in therapeutic hypothermia for perinatal asphyxia. *Pediatrics*,
576 126:e124–e130, 2010.

577 T. J. Hughes. *The Finite Element Method - Linear Static and Dynamic Finites*
578 *Element Analysis*. Prentice-Hall International Editions, New Jersey, 1987.

579 B. R. Kingma, M. J. Vosselman, A. J. Frijns, A. A. Van Steenhoven, and W. D.
580 Van Marken Lichtenbelt. Incorporationg neurophysiological concepts in math-
581 ematical thermoregulation models. *International Journal of Biometeorology*,
582 58(1):87–99, 2014.

583 J. E. Laszczyk and A. J. Nowak. *The analysis of a newborn's brain cooling pro-*
584 *cess - measurements and CFD modelling*. LAP LAMBERT Academic Pub-
585 lishing, Gliwice, 2015a.

586 J. E. Laszczyk and A. J. Nowak. Computational modelling of neonates brain
587 cooling. *International Journal of Numerical Methods for Heat and Fluid Flow*,
588 26(2):571–590, 2015b.

589 G. M. J. Van Leeuwen, J. W. Hand, J. J. W. Lagendijk, D. V. Azzopardi, and
590 A. D. Edwards. Numerical modeling of temperature distributions within the
591 neonatal head. *Pediatric Research*, 48(3):351–356, 2000.

592 A. Nozari, P. Safar, S. W. Stezoski, X. Wu, S. Kostelnik, A. Radovsky, S. Tisher-
593 man, and P. M. Kochanek. Critical time window for intra-arrest cooling with
594 cold saline flush in a dog model of cardiopulmonary resuscitation. *Journal of*
595 *the American Heart Association*, 113:2690–2696, 2006.

596 A. B. C. G. Silva. *Numerical analyses of the temperature distribution in the*
597 *human brain using the finite element method*. MSc dissertation, Federal Uni-
598 versity of Rio de Janeiro, Rio de Janeiro, Brazil, 2012.

599 A. B. C. G. Silva. *A finite element thermoregulation model of the human body for*
600 *hypothermia treatment in adults and neonates*. DSc thesis, Federal University
601 of Rio de Janeiro, Rio de Janeiro, Brazil, 2016.

602 A. B. C. G. Silva, J. Laszczyk, Luiz C. Wrobel, F. L. B. Ribeiro, and A. J.
603 Nowak. A thermoregulation model for hypothermic treatment of neonates.
604 *Medical Engineering and Physics*, 38:988–998, 2016.

605 S. A. Tisherman and F. Sterz. *Therapeutic Hypothermia*. Springer, San Fran-
606 cisco, 2005.

607 National Perinatal Epidemiology Unit. TOBY study protocol - whole body hy-
608 pothermia for the treatment of perinatal asphyxial encephalopathy. volume 2.
609 National Perinatal Epidemiology Unit, 2006.

610 L. J. Vallez, B. D. Plourde, and J. P. Abraham. A new computational thermal
611 model of the whole human body: Applications to patient warming blankets.
612 *Numerical Heat Transfer - Part A*, 69(3):227–241, 2016.

613 H. Wang, W. Olivero, G. Lanzino, W. Elkins, J. Rose, and D. Honings. Rapid
614 and selective cerebral hypothermia achieved using a cooling helmet. *Journal*
615 *of Neurosurgery*, 100:272–277, 2004.

S. Hai Xiang and J. Liu. Comprehensive evaluation on the heating capacities of four typical whole body hyperthermia strategies via compartmental model. *International Journal of Heat and Mass Transfer*, 51:5486–5496, 2008.

Y. Yang, X. Ou, and Q. Chen. A study on time of head hypothermy for large acreage cerebral infarction patients with central high fever. *Chinese Nursery*, 20:45–46, 2006.

L. Zhu and C. Diao. Theoretical simulation of temperature distribution in the brain during mild hypothermia treatment for brain injury. *Medical Biological Engineering Computing*, 39(6):681–687, 2001.

L. Zhu, T. Schappeler, C. Cordero-Tumangday, and A. J. Rosengart. Thermal interactions between blood and tissue. *Advances in Numerical Heat Transfer*, 3:191–219, 2009.